Available online at www.sciencedirect.com
SCIENCE DIRECT®
Journal of Nuclear Materials 328 (2004) 46–54
journal of nuclear materials
www.elsevier.com/locate/jnucmat

Thermal variation of the optical absorption of UO_2: determination of the small polaron self-energy

P. Ruello [a,c,*], K.D. Becker [b], K. Ullrich [b], L. Desgranges [c], C. Petot [a], G. Petot-Ervas [a]

[a] *Laboratoire Structures, Propriétés et Modélisation des Solides, UMR 8580 CNRS/Ecole Centrale Paris, Grande Voie des Vignes, 92295 Châtenay Malabry, France*

[b] *Institut für Physikalische und Theoretische Chemie, Technische Universität Braunschweig, Hans-sommer-Str. 10, D-38106 Braunschweig, Germany*

[c] *Commissariat à l'Energie Atomique, Département d'Etude du Combustible, Centre de Cadarache, 13108 Saint-Paul-Lez-Durance, France*

Received 12 May 2003; accepted 15 March 2004

Abstract

The temperature variation of UV–VIS–NIR optical spectra of UO_2 have been investigated from room temperature up to 1173 K with careful in situ oxygen partial pressure control. The deduced optical absorption edge exhibits a strong temperature dependence. Its value decreases from ~2 eV at room temperature to ~0.8 eV at 1173 K. Such thermal behaviour is interpreted as the consequence of the existence of a strong electron–phonon coupling (small polaron). In the temperature range 300–1173 K, the model yields a hopping radius of ~2 Å and a polaron self-energy of $E_p = -0.38$ eV.

1. Introduction

Uranium dioxide is a typical nuclear fuel used in the pressurised water reactors (PWR). The optimisation of the fuel characteristics, and of the nuclear safety, particularly requires an accurate modelling of the physical and chemical properties of UO_2. This is the reason why many studies and research programs have been devoted to that material. Among the different physical properties, the electrical and thermal properties have received special attention since they exhibit singular behaviour in the vicinity of 1300 K which is the typical temperature of UO_2 pellets in normal PWR operation. Around this range of temperature, it is observed, indeed, that electrical conductivity and heat capacity both present a drastic change in their temperature dependence [1–7]. This abnormal behaviour has been attributed either to the emergence of intrinsic electronic charge carriers [8,9], or to simultaneous electronic and oxygen anti-Frenkel pair disorder [10]. Other authors claim that such an anti-Frenkel defect regime has to be taken into account only for the very high temperature range ($T > 2000$ K) [11,12]. Nevertheless in the range ($T < 2000$ K), the electronic disorder is usually expected to be more important than anti-Frenkel disorder and is therefore considered as the process responsible for the observed variations in the thermophysical properties of UO_2 [8,9,11,13].

The increase of the electrical conductivity, i.e. the electrical transition, has been modelled and, according to many authors [1,2,8,13–16], is driven by the occurrence of electron–hole pairs, which are schematically represented by the following disproportionation reaction $2U^{4+}(5f^2) \Longleftrightarrow U^{3+}(5f^3) + U^{5+}(5f^1)$ [8,16,17]. The

* Corresponding author. Present address: Laboratoire de Physique de l'Etat Condensé, UMR 6087 CNRS/Université du Maine, Avenue Olivier Messiaen, 72085 Le Mans, France.
E-mail address: pascal.ruello@univ-lemans.fr (P. Ruello).

0022-3115/$ - see front matter © 2004 Elsevier B.V. All rights reserved.
doi:10.1016/j.jnucmat.2004.03.002

interpretation of such an electronic defect formation requires the knowledge of the electronic structure of UO_2 which has been determined only recently [18–20] because of the difficulty encountered with the modelling of 5f electrons. It is now proven that UO_2 can be classified as a Mott–Hubbard insulator with an f–f gap [19]. In order to account for the defect formation, UO_2 electronic structure can then be simplified in a two band system as presented in Fig. 1, and can then be described in the framework of the Mott–Hubbard band model [18–21]. This model can be characterized by two energies that can be determined both experimentally and theoretically: U is the energy difference between the centres of the two bands (Fig. 1), E_g is the energy difference between the lower side of the upper band and the upper side of the lower band. The U term is called the Mott–Hubbard gap. Baer and Schoenes [17] have proposed $U \sim 4.6$ eV, Dudarev et al. [21] have suggested $U \sim 4$ eV from an ab initio LSDA + U calculation, Jollet et al. [19] proposed $U \sim 4.8$ eV from both experimental and theoretical results. On the other hand, the minimum formation energy (the gap energy E_g, Fig. 1) has been determined by electrical conductivity measurements. Several studies performed during the last decades have yielded defect formation energies E_g close to 2 eV [1,2,14,15]. Killeen [8] found 1.86 eV, Bates et al. [1] proposed 1.94 eV. Recently, in an electrical conductivity study, we have found a gap of $E_g \sim 2$ eV which confirms the previous results [13]. This gap energy determined from electrical conductivity is in agreement with the band gap deduced from UV–VIS–NIR optical absorption measurements performed in the range 10–300 K [22–24].

It has been strongly suggested by several authors [8,13,18,25–29] that the electronic defects in uranium dioxide move through the crystal by phonon assisted hopping (small polaron mechanism). The analysis of the thermally activated electron and hole mobility in the extrinsic regime (fixed electron or hole concentration) directly provides the migration energy. Devreese et al. [25] and later, Casado et al. [18] have suggested a non-adiabatic hopping process. According to that mechanism, the migration energy E_m was deduced by Devreese et al. [25] to be $E_m = 0.26$ eV, Casado et al. [18] have reported a value of 0.28 eV and we have proposed $E_m = 0.3$ eV [13,30]. Such quite high migration energy clearly suggests a rather deep self-trapping potential and indicates how much the charge carriers couple to the lattice. A few attempts have been undertaken to determine the polaron self-energy and the associated polaron radius [18]. Casado et al. [18] have used the small polaron model of Lang and Firsov [31], where only the nearest neighbours cationic distance ($a_o\sqrt{2} = 3.8$ Å), the static and electronic dielectric properties are required as external parameters. They found a polaron self-energy (E_p) of −0.8 eV and a polaron radius of 3.8 Å.

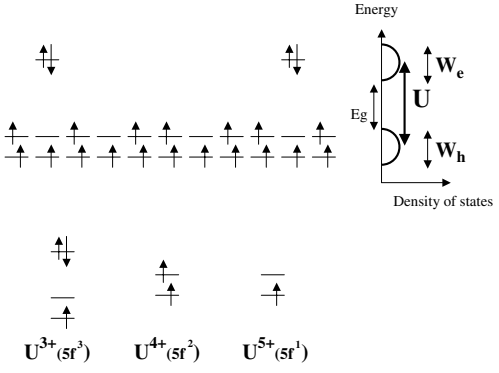

Fig. 1. Mott–Hubbard insulating state of UO_2 (U = intra-orbital coulombic repulsive energy, W_h and W_e represent schematically the lower and upper Hubbard band. Assuming $W_e \sim W_h$, the band gap is $E_g = U - W$).

In the present paper, we aim at characterizing experimentally the polaron self-energy by optical studies. Considering the well known deep influence of the polaron on the absorption edge [32–36], we are able to give an estimation of the small polaron self-energy thanks to UV–VIS–near IR measurements performed as a function of temperature. The mechanism of polaron formation, indeed, usually involves the coupling between the electronic defects and the longitudinal optical modes (LO) in polar compound and specially in oxides. Such coupling allows phonon assisted optical transition and, thus, enhances light absorption in the range $h\upsilon \lesssim E_g$. The phonon assisted transition probability is related to the distribution of LO phonons, which according to the Bose–Einstein distribution, is an increasing function of temperature. Therefore, the band edge shifts to lower energy with rising temperatures. Moreover, the band edge shift is all the more important than the electron–phonon coupling is large [32]. This effect has already been observed in the literature for oxides [32,33] or polar semiconductors [35,36]. A red shift of the UO_2 gap was observed by Schoenes [22] from 5 to 300 K and has been attributed to phonon assisted optical transition. The study of Griffiths et al. [23,24] has also revealed a large red shift of the absorption edge (gap) from 85 to 985 K. They report a gap decrease of ~0.4 eV from 85 to 985 K. Such quite large variation, typical to oxides [32,33], halides [34], and polar semiconductor [35,36], indicates that the electron–lattice interaction is important in UO_2 as expected because we know polaron actually exist.

In this study, optical absorption was measured in transmission geometry with variable temperatures ranging from 300 K up to 1173 K. Controlled thermochemical conditions were systematically applied at each temperature to ensure the exact stoichiometry, O/U = 2. A modelling of the thermal variation of the absorption

edge is used for having an estimate of the polaron radius and its self-energy. We finally discuss the localized states and the polaron band in UO_2.

2. Experiment

2.1. Sample preparation and characterization

A piece of a single crystal was thinned down to 30 μm and then polished. No particular crystallographic orientation was chosen. The thin single crystal (area of 3×3 mm^2), transmits only red light at room temperature, which is consistent with a band gap of ~2 eV.

The defect concentration was measured as given in Table 1.

2.2. Measurements

The thin sample was carefully placed into a thin slit of an alumina sample holder. The sample covered completely the aperture. The quartz windows are hold and sealed by a water cooled frame. Their temperature is below 200 °C.

In the UV–VIS–NIR spectral range, the optical absorption of a thin absorber with parallel faces is determined according to [37]:

$$\alpha = \frac{\log\left(\frac{I_o}{I_t}\right)}{e} + \frac{2\log(1-R)}{e}, \tag{1}$$

where I_o, I_t, and e are the incident light intensity, the transmitted intensity, and the sample thickness. In the UV–VIS–NIR range, only the electronic part of the dielectric constant is taken into account. As a consequence, the reflectivity R is given by the following relation:

$$R = \frac{(\sqrt{\varepsilon_\infty}-1)^2}{(\sqrt{\varepsilon_\infty}+1)^2}, \tag{2}$$

where $\varepsilon_\infty = 5$ is the electronic dielectric constant [22].

The ratio I_o/I_t cannot be measured directly because of the black body radiation which cannot be neglected for temperatures above 500 K. Therefore, in order to make allowance of this black body radiation, two in situ measurements are required. The first gives the total apparent absorbance (A_B) which is:

$$A_B = \log\left(\frac{I_o}{I_t + I_{bb}}\right), \tag{3}$$

where I_o, I_t and I_{bb} are the incident and the transmitted light intensity, and the intensity due to black body radiation, respectively. The corresponding experimental set-up is schematically represented on Fig. 2(a).

The second measurement is restricted to the black body radiation I_{bb} exclusively (Fig. 2(b)). For this, we mask the incident light to prevent it from going through the sample. We get then A_{bb}:

$$A_{bb} = \log\left(\frac{I_o}{I_{bb}}\right) \tag{4}$$

Finally, the absorbance (I_o/I_t) is obtained according to the following expression:

$$A_t = A_B + A_{bb} - \log(10^{A_{bb}} - 10^{A_B}) = \log\left(\frac{I_o}{I_t}\right). \tag{5}$$

As a comparison, the absorption spectrum measured with and without the black body contribution is displayed in Fig. 3. A comparison of the experimental black body radiation intensity and the theoretical one (Eq. (6) [38]) is also displayed showing the reliability of the measurements.

Table 1
Prevailing impurities in the urania single crystal

Elements	Amount (ppm)
Fe	560
Mn	155
Ca	123
V, Pb	10
K, Mg, P, Al, Ti, Cr, Cu, Zn, Zr, Nb, W, Th	⩽6

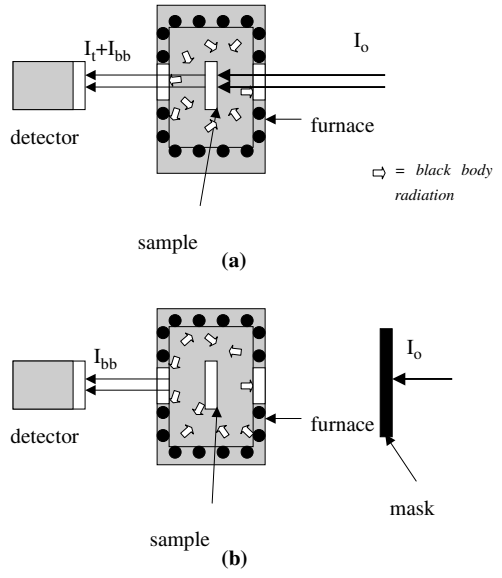

Fig. 2. Experimental set-up. (a) Optical measurement of transmitted light including the black body radiation contribution, (b) optical measurement of the black body radiation contribution alone.

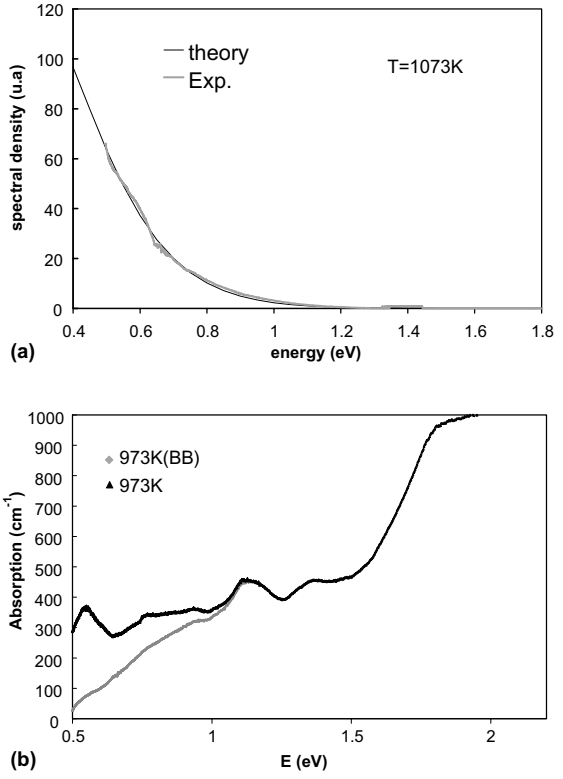

Fig. 3. Spectral density of the black body radiation. (a) Comparison between theory and experimental measurement, (b) comparison of the absorption spectrum with (973 K) and without (973 K (BB)) making allowance of the black body radiation.

$$u(w,T) = \frac{\hbar}{\pi^2 c^3} \frac{w^3}{e^{(\hbar w/kT)} - 1}. \quad (6)$$

In our measurement the black body radiation of our furnace seems to be larger than that of Griffiths et al. [24] because, we can clearly distinguish the absorption peaks around 0.5 eV only after making allowance of the black body. Consequently, it appears that the resolution of the fine structure in the range 0.5–1 eV is more difficult in our study. As we already mentioned in Section 1, we only focus on the gap region in this paper.

The measurements were performed using a Perkin–Elmer Lambda 9 spectrometer (from the Institut für Physikalische und Theroretische Chemie, TU Braunschweig) which allows in situ high temperature measurements, up to 1500 K [39,40]. A thermocouple is placed in the vicinity of the sample. Special thermochemical conditions ensuring exact stoichiometry were used according to literature [13,30,41,42]. In the present study, the adequate in situ oxygen partial pressure was buffered by a chosen flowing CO/CO_2 gas mixture that had been diluted by N_2. The oxygen partial pressure imposed versus temperature is displayed in Fig. 4. The

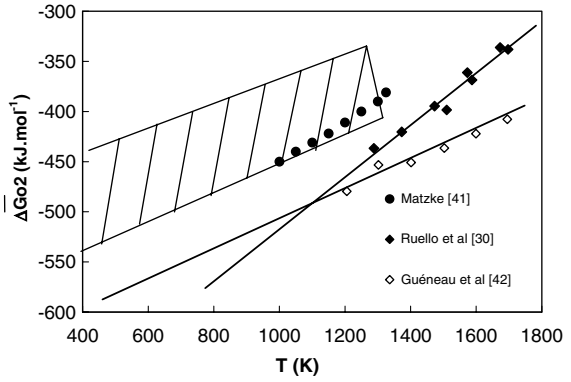

Fig. 4. Oxygen partial pressure imposed around the sample during spectroscopy study (dashed region). Comparison with recent new thermodynamical data of stoichiometric UO_2 [30,41,42].

measurements of the optical absorption were performed for nine temperatures between 293 and 1173 K. Cycling temperature procedure was adopted as to insure the reliability of the measurements.

3. Thermal variation of the absorption edge

The optical absorption spectra are plotted in Fig. 5. In agreement with the study by Schoenes [22] and Griffiths et al. [23,24], we observe at room temperature a strong light absorption occurring for incident light energies higher than 1.9/2 eV: this corresponds to the so-called gap (E_g).

As already pointed out in Section 1, the absorption edge (1.9/2 eV) is in agreement with the band gap determined from electrical conductivity. For the room temperature spectrum, the phonons cannot drastically affect the band edge because the Bose–Einstein occupation numbers of the LO modes is rather small. Only a

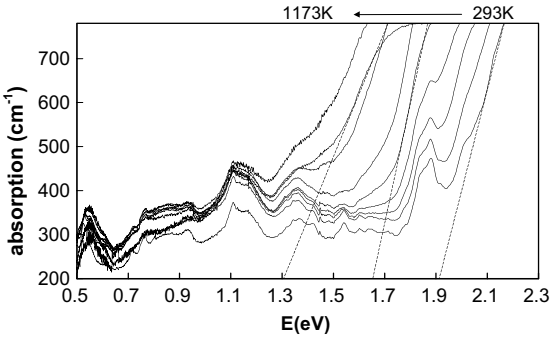

Fig. 5. Thermal variation of the UV–VIS–NIR absorption spectrum of a thin (30 μm) UO_2 single crystal.

small shift to the lower energy of the absorption edge was reported from 85–100 K to 300 K ($\Delta E_g(T) \sim 0.05$ eV) [22–24]. This situation contrasts with that in the range 300–1173 K, where the onset of the optical absorption shifts drastically to lower energies. We can estimate the onset of the absorption edge ($E_g(T)$) by extrapolating the spectral feature from the higher-energy side as indicated by the dashed lines shown in Fig. 5. The chosen base line of the absorption (200 cm^{-1}) is larger than that calculated from the reflectivity contribution (40 cm^{-1}). This may, probably, be due to light scattering processes which may occur at a non-perfect polished surface. Nevertheless, if we compare our results, at room temperature, with those of Schoenes [22], one can observe that between 0.5 and 2.1 eV the absorption levels are in agreement and the fine structures below the absorption edge revealed by Schoenes are also observed in our studies. These same fine structures are also found in the work of Griffiths et al. [23,24]. Nevertheless, in their study, the absorption level, in the range 0.5–2 eV increases more strongly with energy than in our experiment. From 0.5 to 1.9 eV, the increase of the absorption level is ~1700, ~400 and ~400 cm^{-1} for Griffiths et al. [23,24], Schoenes [22] and our work. These several small peaks are attributed to 5f(U) crystal field transitions by the previous authors [22–24]. Because we have well controlled the oxygen partial pressure in equilibrium with the sample, it is reasonable to consider such fines structure as intrinsic to the UO_2 solid and not related to eventual variation of stoechiometry as advocated by Schoenes [22]. In Fig. 6, the absorption edge energy ($E_g(T)$) is plotted as a function of temperature together with values due to Schoenes [22] and Griffiths et al. [24]. The qualitative thermal variation reported by Griffiths et al. and our experiment are in agreement. The difference between the absolute values is because values of Griffiths et al. [24] correspond to a constant absorption (4000 cm^{-1}) while ours are determined as mentioned above and are more likely directly related to the gap. This thermal variation is classical and very similar to that of classical semiconductors such as Ge [35] and InP and GaAs [36] and oxides [33]. In each system the shift of the absorption edge between 300 and 1000 K is large and is ~0.3, ~0.35 and ~0.6 eV for InP, GaAs and UO_2 respectively. Such large variation is usually associated to large electron–phonon coupling due to the polar nature of the lattice, as discussed in the following section.

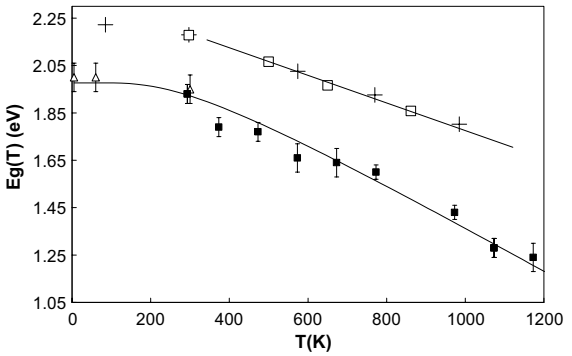

Fig. 6. Thermal variation of the optical absorption edge of UO_2. The full black square: this work, the empty triangle [22], the empty square and the cross [24]. The solid line added to our data corresponds to the fitted data taking into account the coupling between LO-phonon and charge carriers.

3.1. Modelling of electron–lattice coupling

In the temperature range 300–1173 K, the thermal band gap ($E_g(T)$) is a linear decreasing function of temperature which can be empirically described by the formulation proposed by Kröger [34]:

$$E_g(T) = a - bT. \tag{7}$$

From the plot shown in Fig. 6, a rough calculation, performed between 400 and 1173 K, leads a b-value of $b = 8 \times 10^{-4}$–9×10^{-4} eV K^{-1}, which is in agreement with other values reported in the literature. Kröger [34] cited a typical range of 7.5×10^{-4}–27×10^{-3} eV K^{-1} for oxides and ionic compounds. More recently, a similar temperature dependence has been reported for La_2CuO_4 with $b = 6.8 \times 10^{-4}$ eV K^{-1} [33].

At constant pressure, which is the present thermodynamical condition, the absorption edge is a function of volume V and of temperature T. A variation of the absorption edge assumes then the following expression [35]:

$$\Delta E_g = \left(\frac{\partial E_g}{\partial V}\right)_T \left(\frac{dV}{dT}\right)_P \Delta T + \left(\frac{\partial E_g}{\partial T}\right)_V \Delta T. \tag{8}$$

The first term corresponds to the band gap volume dependence which characterizes the effect of thermal expansion on the orbitals overlapping. The second term is the result of electron–phonon coupling. In polar compounds, such as UO_2, the first one is expected to have a small impact compared to the second term. Therefore, we assume in the following that the phonon interaction contribution is the main mechanism which drives the absorption edge thermal dependence.

These phonon assisted optical transitions, which depend on the strength of the electron–phonon coupling α_p, cause a shift of the band edge which can be described as follows [32,33]:

$$\Delta E_g(T) = E_g(T) - E_g^o = -2\hbar w_o \alpha_p [n(\hbar w_o/kT) + 1], \tag{9}$$

where $n(\hbar w_o/kT)$ is the Bose–Einstein occupation number of the LO mode and E_g^o is the bare band gap which

differs from the effective band gap ($E_g(T)$) by the total electron and hole polaron self energy, $E_g^o - 2\alpha_p\hbar w_o$ is known as the electron–lattice interaction renormalized band gap [35]; and α_p is the coupling parameter which according to [32,33,43,44] is given by

$$\alpha_p = \frac{1}{2}\frac{e^2}{2\hbar w_o 4\pi\varepsilon_o}\left(\frac{1}{\varepsilon_\infty}-\frac{1}{\varepsilon_S}\right)\left(\frac{2mw_o}{\hbar}\right)^{1/2}, \quad (10)$$

where ε_S and ε_∞ are the static dielectric constant and the electronic contribution, respectively. The last term is the inverse of the polaron radius, r_p:

$$r_p = \left(\frac{\hbar}{2mw_o}\right)^{1/2}. \quad (11)$$

This formulation only takes into account an effective frequency of LO phonons (w_o), which is considered as the main interacting mode [31–33].

In this model, it is assumed that the electron and hole have the same effective mass and hence the same coupling parameter. For UO_2, the first condition appears to be consistent with results derived from high temperature thermoelectric power experiments which yielded $m_e^* \approx m_h^*$ [13,30]. In previous work [13], in agreement with Hyland et al. [8], it has also been shown that $\mu_n \sim \mu_p$ which means that electrons and holes possess the same migration energy and, hence, similar hopping rates. In the small polaron theory of Lang and Firsov [31], and also as pointed out by Casado et al. [18], the activation energy is directly related to the coupling parameter. Therefore, owing to the equality between the n-type and p-type activation energy, it is reasonable to assume that α_p and α_n are of similar magnitude.

The LO phonon frequency in UO_2, determined by inelastic neutron scattering [12,45], is $w_o = 1.7 \times 10^{13}$ Hz, corresponding to an LO mode energy of $\hbar w_o = 70$ meV. The model proposed above, Eq. (9), possesses only two adjustable parameters: α_p and E_g^o. In Fig. 6, the solid line represents the best fit by this model. As seen, reasonable agreement is achieved up to 1173 K by using a coupling parameter of $\alpha_p = 5.5$ and a bare band gap of $E_g^o = 2.75$ eV. Thus, we easily deduce the UO_2 gap:

$$\Delta H_f = E_g(0\ \mathrm{K}) = E_g^o - 2\alpha_p\hbar w_o \cong 2\ \mathrm{eV}. \quad (12)$$

Using tabulated values [22] of $\varepsilon_S = 21.5$ and $\varepsilon_\infty = 5$, we also can deduce from the coupling parameter α_p the polaron radius:

$$r_p \sim 2.3\ \text{Å}. \quad (13)$$

It is to be noted that this characteristic length is of the order of the nearest neighbour U–U distance $\left(a_o\sqrt{2} = 3.8\ \text{Å}\right)$ in the crystal, which indicates the strong charge carrier localization. This polaron radius value yields to a quasi-particle effective mass of $\sim 13\ m_e$ which illustrates the small charge carrier mobility. Finally, we can estimate the polaron self-energy defined as $E_p = -\alpha_{p\hbar} w_o$, and obtain:

$$E_p = -\alpha_p\hbar w_o = -0.38\ \mathrm{eV}. \quad (14)$$

This value is smaller by a factor of 2 than that calculated by Casado et al. [18], who proposed a value of $E_p = -0.8$ eV. This discrepancy will be discussed later. In the framework of polaron modelling, an absorption peak is expected at $2E_p$ and $4E_p$ for a single and bipolaron respectively. In the work of Griffiths et al. [23,24], a peak at $\sim$0.78 eV was evidenced and exhibits similitude with the energy $2E_p = 0.76$ eV deduced from our experimentally determined E_p value. Nevertheless, such comparison must be carefully considered because Griffiths et al. have detected this peak in UO_{2+x} with $x > 0.035$ which corresponds to a stoichiometric range where Willis clusters are formed [29]. Moreover, it is not clear yet which of single polaron or bipolaron actually are formed.

3.2. Tests on polaron description self consistency

The physical features of the polaron in UO_2 determined in the present experimental study support the localization of the charge carrier. This is consistent with the analysis of the electron–hole transport properties discussed in Section 1 and in Refs. [18,25,30]. We can discuss this localization assumption by comparing the polaron self-energy with the overlap integral J which can be deduced from our electrical conductivity measurements and also by calculating the criterion value (η_d) for nearest-neighbours hopping processes.

The first criterion that a single charge carrier must fulfil to form a small polaron is that the lattice coupling energy (E_p), must exceed the energy achieved by delocalization into an extended Bloch state. A localized state must be created below the bands W_e or W_h respectively for the electron and the hole. In the following, we will assume W_e and W_h to be the same ($W = W_e = W_h$) (Fig. 1). Consequently, this condition is given by

$$|E_p| > W/2 = zJ. \quad (15)$$

Here, z is the number of nearest neighbour cations ($z = 12$ for the fluorite of UO_2) and J is the resonant transfer integral between two nearest neighbours.

The second criterion to be fulfilled is defined, for nearest-hopping [31], by $\eta_d \ll 1$.

$$\eta_d = \frac{J}{E_m}\frac{J}{kT} \ll 1. \quad (16)$$

The first term of (16) is the ratio between the time of tunnelling $\left(t_B \sim \frac{\hbar}{J}\right)$ and the time of hopping $\left(t_H \sim \frac{\hbar}{E_m}\right)$: E_m is the migration energy. The second is the ratio between the time of tunnelling and the characteristic time

of thermal fluctuation ($t_T \sim \frac{\hbar}{kT}$). Both these ratios must be smaller than 1. The first inequality ($t_H/t_B < 1$) means that, for a nearest hopping, the hopping time must be shorter than the tunnelling time. The second condition ($t_T/t_B < 1$) means that the tunnelling time must be longer than the time between two thermal fluctuations which allow multiphonon transition and then hopping via phonon assisted migration [26,31].

In order to perform these estimations, we first determine the overlap integral J of the upper or lower Hubbard band, respectively, for the electron type charge carrier (U^{3+}) or the hole type charge carrier (U^{5+}) (Fig. 1). The value of the overlap integral is deduced from an analysis of the electrical conductivity assuming the non-adiabatic mechanism proposed by Devreese et al. [25], Coninck et al. [28] and later by Casado et al. [18]. In this case, the electrical conductivity has the following temperature dependence [31]:

$$\sigma = \left(\frac{\sigma_o}{T^{3/2}}\right) \exp\left(-\frac{E_m}{kT}\right), \tag{17}$$

where

$$\sigma_o = \frac{2ne^2J^2}{ka_o\hbar}\sqrt{\frac{\pi}{kE_m}}, \tag{18}$$

n denotes the ratio between the concentration of mobile charge carriers and of the concentration of cations. E_m is the activation energy for drift mobility ($E_m = 0.3$ eV). The others symbols have the usual meaning.

From our results for the extrinsic regime [13], where

$$\sigma = \left(\frac{1.14 \times 10^7}{T^{3/2}}\right) \exp\left(-\frac{0.3 \text{ eV}}{kT}\right),$$

we can determine σ_o. Using the mobility at 1073 K reported by Dudney et al. [29] ($\mu = 1.9 \times 10^{-2}$ cm^2 V^{-1} s^{-1}) and considering our electrical conductivity value of 12.5 S m^{-1} for this temperature, we can estimate the concentration of ionised impurities. We obtain $C_n \sim 4 \times 10^{25}$ m^{-3} ($n = C_n/C_U \sim 2 \times 10^{-3}$) and thus obtain $J = 0.04$ eV. It is to be noted, however, that the charge carrier mobility was not directly measured but deduced from a mobility analysis of a Y_2O_3 doped material [29]. Therefore, some caution has to be applied. If we consider all the impurities detected in our sample (see Table 1) to be fully ionised, we get a charge carrier amount of $n \sim 8 \times 10^{-3}$ and deduce a J-value of 0.02 eV.

Thus, depending on the estimation of the ionised impurities (Eqs. (17) and (18)), we finally arrive at an estimated range of J:

$$0.02 \text{ eV} < J < 0.04 \text{ eV}. \tag{19}$$

This J value is in reasonable agreement with results reported by Casado et al. [18], who proposed $0.04 \text{ eV} \leqslant J \leqslant 0.056$ eV on basis of an estimation of the ionised impurities in the electrical conductivity data of Bates et al. [1].

With this value of the overlap integral one can confirm first that small polaron states actually tend to be energetically more favoured because η_d (16) is indeed smaller than 1 over the whole temperature range $T > 300$ K. One can also demonstrate that the criterion for the non-adiabatic polaron, Eq. (20), is actually fulfilled in the investigated temperature range ($T > 300$ K) [18,31].

$$\eta_a = \frac{J^2}{\hbar\omega_0\sqrt{E_m kT}} \ll 1. \tag{20}$$

Nevertheless, according to our J values, the dip in the polaron level does not systematically exceed the width of the resonant transfer band. Depending on the two cases (1) and (2) depicted in Fig. 7, the calculation shows that one either finds a small polaron mechanism or an extended like state.

Casado et al. [18], who calculated a polaron energy by theoretical calculation, fulfilled the criterion (15) with a value of $E_p = -0.8$ eV. On the other hand, we conclude that the experimental study does not lead so easily to a consistent model because it suggests that extended states could exist (case 2). Case 2, of course, is not consistent with the electron–lattice mechanism described above where the thermally activated charge carrier mobility and the small polaron radius (r_p), indeed, supported the small polaron mechanism in UO_2.

The problem clearly points out the difficulty in reconciling the features (E_p) deduced from optical measurements with those from electrical conductivity (J). We think that one of the reasons why we find a case $zJ > |E_p|$ could probably arise from an incorrect determination of J. J is indeed not directly measured and is

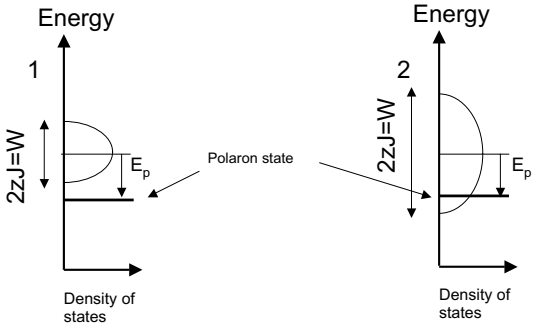

Fig. 7. Schematic representation of the polaron self-trapping well and the resonant transfer band $2zJ$ (z is the nearest neighbours number). Two cases are presented (1) $J = 0.02$ eV, (2) $J = 0.04$ eV. Only the first case is compatible with polaron formation (existence of a localized state below the band).

completely dependent on the concentration of ionised impurities which is rather difficult to know. If we consider the values determined in literature for U [17,19–21], we find lower ($U = 4$ eV) and a upper ($U = 4.8$ eV) limits. Together with our J values we obtain the following estimate for the gap energy, according to the definition of the Mott–Hubbard gap and in the approximation $W_e \sim W_h$:

$$3.04 \text{ eV} < E_g = U - W < 4.14 \text{ eV}. \quad (21)$$

This range is not consistent with the experimental value, $E_g \sim 2$ eV, (electrical conductivity and optical measurements). A larger value for J would improve the agreement between the experimental Mott–Hubbard gap and that deduced from $E_g = U - W$. However, an increase of J can easily lead to a violation of the criterion (14).

Further investigations are required to better characterize U, the overlap integral, and the polaron band. The model adopted here to deduce electron–phonon features could be improved by including more than one phonon for example. Moreover, one should try to estimate the effect of thermal expansion (7) on the band gap shift.

For that, the knowledge of $\left(\frac{\partial E_g}{\partial V}\right)_P$ is required but not available yet. Furthermore, as pointed out by Casado et al. [18], the value of J derived from electrical conductivity implies, as an approximation, that the entire conductivity is governed by small polarons. Sumi [46] suggests, indeed, that large polarons, with non-activated mobility, could also contribute to the electrical conductivity of oxides. In that case, J could probably be overestimated in the present case and merely represents an upper limit.

4. Conclusion

In this paper we have measured the optical absorption of a thin UO_2 single crystal between 300 and 1173 K. Our results are pretty in agreement with literature. The low-energy shift of the band edge with increasing temperatures has been related to phonon assisted electronic transition processes. The electron–phonon interaction was described in the framework of the small polaron model and the radius and self-energy of the polaron in UO_2 have been estimated: $r_p \sim 2.3$ Å, $E_p = -0.38$ eV. These polaron features have been found to be consistent with a small polaron state suggested in our previous electrical conductivity study and also with theoretical calculations reported in the literature. Nevertheless, the poor determination of the amount of ionised impurities prevents an accurate determination of the resonance transfer energy J which would be valuable for a accurate modelling of the polaron state.

Acknowledgements

The authors are grateful to F. Schrobsdorff for her help in the experiment and to T. Petit and L. Caillot for fruitful discussions. This work was supported by the CEA.

References

[1] J.L. Bates, C.A. Hinman, T. Kawada, J. Am. Ceram. Soc. 50 (12) (1967) 652.
[2] R.N. Hampton, G.A. Saunders, A.M. Stoneham, J.H. Harding, J. Nucl. Mater. 154 (1988) 245.
[3] M.G. Chasanov, L. Leibowitz, S.D. Gablenick, J. Nucl. Mater. 49 (1973/74) 129.
[4] J.F. Kerrisk, D.G. Clifton, Nucl. Technol. 16 (1972) 531.
[5] R. Szwarc, J. Phys. Chem. Sol. 30 (1969) 705.
[6] R.A. Hein, L.H. Sjodahl, R.J. Szwarc, J. Nucl. Mater. 25 (1968) 99.
[7] J.P. Hiernaut, G.J. Hyland, C. Ronchi, International Journal of Thermophysics 14 (2) (1993).
[8] G.J. Hyland, J. Ralph, High Temp. High Press. 15 (1983) 179.
[9] P. Browning, J. Nucl. Mater. 98 (1981) 345.
[10] K. Naito, T. Tsuji, T. Matsui, in: J. Nowotny, W. Weppner (Eds.), Grain Boundaries and Structural Defects, Kluwer Academic, 1989, p. 27.
[11] J.K. Fink, J. Nucl. Mater. 279 (2000) 1.
[12] M.T. Hutchings, J. Chem. Soc. Faraday Trans. 2 83 (1987) 1083.
[13] P. Ruello, PhD thesis Ecole Centrale des Arts et Manufactures, Ecole Centrale Paris, No. 2001-35, 2001.
[14] J.C. Killeen, J. Nucl. Mater. 88 (1980) 185.
[15] J.C. Killeen, J. Nucl. Mater. 92 (1980) 136.
[16] C.R.A. Catlow, Proc. R. Soc. Lond. A 353 (1977) 533.
[17] Y. Baer, J. Schoenes, Solid State Commun. 33 (1980) 885.
[18] J.M. Casado, J.H. Harding, G.J. Hyland, J. Phys. Condens. Matter 6 (1994) 4685.
[19] F. Jollet, T. Petit, S. Gota, N. Thromat, M. Gautier-Soyer, A. Pasturel, J. Phys.: Condens. Matter 9 (1997) 9393.
[20] Z.Y. Wu, F. Jollet, S. Gota, N. Thromat, M. Gautier-Soyer, T. Petit, J. Phys.: Condens. Matter 11 (1999) 7185.
[21] Dudarev, Philos. Mag. B 75 (5) (1997) 613.
[22] J. Schoenes, Phys. Rep. 63 (6) (1980) 301.
[23] T.R. Griffiths, H.S.St.A. Hubbard, M.J. Davies, Inorg. Chem. Acta 225 (1994) 305.
[24] T.R. Griffiths, H.V.St.A. Hubbard, J. Nucl. Mater. 185 (1991) 243.
[25] J. Devreese, R. De Coninck, H. Pollack, Phys. Status Solidi 17 (1966) 825.
[26] J.T. Devreese, in: "Polarons" Encyclopedia of Applied Physics, 14, Wiley-VCH, 1996, p. 383.
[27] J. Devreese, Bull. Soc. Belge Phys. Sér. III (1963) 259.
[28] R. De Coninck, J. Devresse, Phys. Status Solidi 32 (1969) 823.
[29] N.J. Dudney, R.L. Coble, H.L. Tuller, J. Am. Ceram. Soc. 64 (11) (1981) 627.
[30] P. Ruello, G. Petot-Ervas, C. Petot, L. Desgranges, J. Am. Cer. Soc., in press.
[31] I.G. Lang, Yu.A. Firsov, Sov. Phys. JETP 16 (5) (1963) 1301.

[32] H.Y. Fan, Phys. Rev. 82 (1951) 900.
[33] J.P. Falck, A. Levy, M.A. Kastner, R.J. Birgenau, Phys. Rev. Lett. 69 (7) (1992) 1109.
[34] F.A. Kröger, V.J. Vink, in: F. Seitz, D. Turnbull (Eds.), Solid State Physics, vol. 3, Academic Press, New York, 1956, p. 307.
[35] P.Y. Yu, M. Cardona, Fundamentals of Semiconductors, 3rd Ed., Springer-Verlag, 2001 (ISBN 3-540-41323-5).
[36] M. Beaudoin, J.G. DeVries, S.R. Johnson, H. Laman, T. Tiedje, Appl. Phys. Lett. 70 (26) (1997) 3541.
[37] H. Kuzmani, Solid State Spectroscopy, Springer-Verlag, Berlin, Heidelberg, 1998.
[38] B. Diu, C. Guthman, D. Lederer, B. Roulet, Physique statistique, Hermann Editeurs des sciences et des arts, 1989.
[39] K.D. Becker, Philos. Mag. A 68 (4) (1993) 767.
[40] K.D. Becker, Ber. Bunsenges. Phys. Chem. 101 (9) (1997) 1248.
[41] Hj. Matzke, J. Nucl. Mater. 208 (1994) 18.
[42] C. Guéneau, M. Baichi, D. Labroche, C. Chatillon, B. Sudman, J. Nucl. Mater. 304 (2002) 161.
[43] N. Tsuda, K. Nasu, A. Fujimori, K. Siratori, Electronic Conduction in Oxides, Solid-State Sciences, 2nd Ed., Springer, 2000.
[44] H. Fröhlich, H. Pelzer, S. Zienau, Philos. Mag. 41 (1950) 221.
[45] G. Dolling, R.A. Cowley, A.D.B. Woods, Can. J. Phys. 43 (1965) 1397.
[46] H. Sumi, J. Phys. Soc. Jpn. 33 (1972) 327.